mathematics

MDPI

Article

Adapting the Formula for Planar Spiral Inductors' Inductance Computation to the New Oval Geometric Shape, Ideal for Designing Wireless Power Transfer Systems for Smart Devices

Claudia Pacurar [1,*], Vasile Topa [1], Claudia Constantinescu [1,2], Calin Munteanu [1], Marian Gliga [1,2], Sergiu Andreica [1,2] and Adina Giurgiuman [1,2,*]

[1] Department of Electrotechnics and Measurements, Faculty of Electrical Engineering, Technical University of Cluj-Napoca, 26-28 G. Baritiu Street, 400027 Cluj-Napoca, Romania
[2] Academy of Romanian Scientists, Ilfov 3, 050044 Bucharest, Romania
* Correspondence: claudia.pacurar@ethm.utcluj.ro (C.P.); adina.giurgiuman@ethm.utcluj.ro (A.G.)

Abstract: The most used spiral inductors, in the available scientific literature and in our research activities, so far, have been those with square, hexagonal, octagonal, and circular geometric shapes. Geometry plays an important role in the efficiency of these inductors when used in wireless power transfer. In this article, a new geometric shape is designed by combining the square and the circle to create an oval shape of a planar spiral inductor. Inductors with this new shape are designed, numerically modelled, and practically constructed for experimental testing. The formula for inductance computation for planar spiral inductors is adapted for this new oval shape. New geometric coefficients, required for inductance computation formula, have been determined. The new formula for inductance computation is validated both analytically, by comparing the results with those from numerical modelling, and experimentally, by comparing with measurements, for a wide range of oval spiral inductors. Five sets of different oval spiral inductors are optimally designed, numerically modelled, practically constructed, and experimentally tested. By designing this new shape for planar spiral inductors, the inductance is increased 2.16 times compared to square, 1.84 times compared to hexagonal, 2.12 times compared to octagonal, and 2.52 times compared to circular shapes. The new oval spiral inductor design will be very useful for constructing wireless power transfer systems for pacemakers, smartphones, smartwatches, and/or any other type of smart device.

Keywords: spiral inductor; oval shape; inductance formula; optimal design; numerical modelling; planar electromagnetic technology; geometrical coefficients; experimental measurements

MSC: 00A79

check for updates

Academic Editor: Jacques Lobry

Received: 27 November 2024
Revised: 14 January 2025
Accepted: 20 January 2025
Published: 22 January 2025

Citation: Pacurar, C.; Topa, V.; Constantinescu, C.; Munteanu, C.; Gliga, M.; Andreica, S.; Giurgiuman, A. Adapting the Formula for Planar Spiral Inductors' Inductance Computation to the New Oval Geometric Shape, Ideal for Designing Wireless Power Transfer Systems for Smart Devices. *Mathematics* **2025**, *13*, 348. https://doi.org/10.3390/math13030348

Copyright: © 2025 by the authors. Licensee MDPI, Basel, Switzerland. This article is an open access article distributed under the terms and conditions of the Creative Commons Attribution (CC BY) license (https://creativecommons.org/licenses/by/4.0/).

1. Introduction

In today's world, electromagnetic planar components have become the preferred choice for smart devices, as they are the most used to make devices as small, light, reliable, thin, and high-performing as possible.

Today, there is a growing demand for high-performance smart devices that can be wirelessly powered in a quick and easy manner. Therefore, the optimal design of their components is crucial for achieving high-performance devices. In the literature, there are planar spiral inductors used for VHF [1,2] and RF application [3–5], wave application [6], wireless systems [7–14], implantable systems [15,16], filters [17–19], and antennas [20,21].

In article [9], we designed and constructed a wireless power supply system for small devices, such as pacemakers, using planar spiral inductors, using two common shapes of planar spiral inductors, without optimizing the shapes to maximize the use of the available area of the device to increase the inductance of the inductor and the wireless system performances. To achieve this goal, we analyzed and extracted the inductance of an elliptical spiral inductor [16], but its inductance did not increase significantly, and its geometry did not fit the pacemaker's shape properly.

Therefore, we designed a new shape, an oval spiral inductor, that perfectly matches the pacemaker's shape. This article demonstrates that by designing planar spiral inductors in this new shape, we significantly increased the inductance compared with conventional shapes. The contributions of this article significantly advance the current state of the art in planar inductor design and wireless power transfer (WPT) by addressing key limitations and enhancing performance. The introduction of the oval shape inductor offers improved inductance characteristics compared to conventional shapes. This design optimizes space and allows for better integration in compact WPT systems, leading to more efficient power transfer and potentially smaller device sizes. A new formula for inductance is achieved by adapting previous ones. By adapting the formula for the average diameter and fill ratio, the authors provide a more accurate method to model and predict the behaviour of oval shape inductors. This enhances the precision of inductance calculations, which is crucial for designing high-performance inductors in both low- and high-frequency applications. The introduction of new geometric coefficients accounts for the unique properties of the oval shape, ensuring that inductance is calculated more accurately. This refinement allows for better design optimization, resulting in more efficient inductors and improved overall performance in WPT systems. Together, these contributions enable more efficient and accurate inductor designs, improving the performance of WPT systems, especially in terms of power efficiency, size reduction, and integration capabilities, which are essential for advancing the technology in modern applications.

2. Planar Spiral Inductors with Square, Hexagonal, Octagonal, and Circular Shapes

Until a few years ago, the most used shapes for planar spiral inductors were square, hexagonal, octagonal, and circular. Formulas for extracting spiral inductor parameters and software programs were developed by the authors in [22,23], but only for these four conventional shapes shown in Figure 1.

A variety of formulas can be found in the literature [22–31] for calculating the inductance of planar spiral inductors with these geometric shapes. The most accurate expression, explicitly derived for these four shapes, is provided in [25]:

$$L_{spiral\ planar\ inductor} = \frac{\mu N^2 d_{avg} C_1}{2}\left[\ln\left(\frac{C_2}{\rho}\right) + C_3\rho + C_4\rho^2\right], \quad (1)$$

where

- N is the number of turns;
- d_{avg} is the average diameter:

$$d_{avg} = \frac{d_e + d_i}{2}, \quad (2)$$

- d_e is the outer diameter;
- d_i is the inner diameter;
- ρ is the fill factor:

$$\rho = \frac{d_e - d_i}{d_e + d_i}, \tag{3}$$

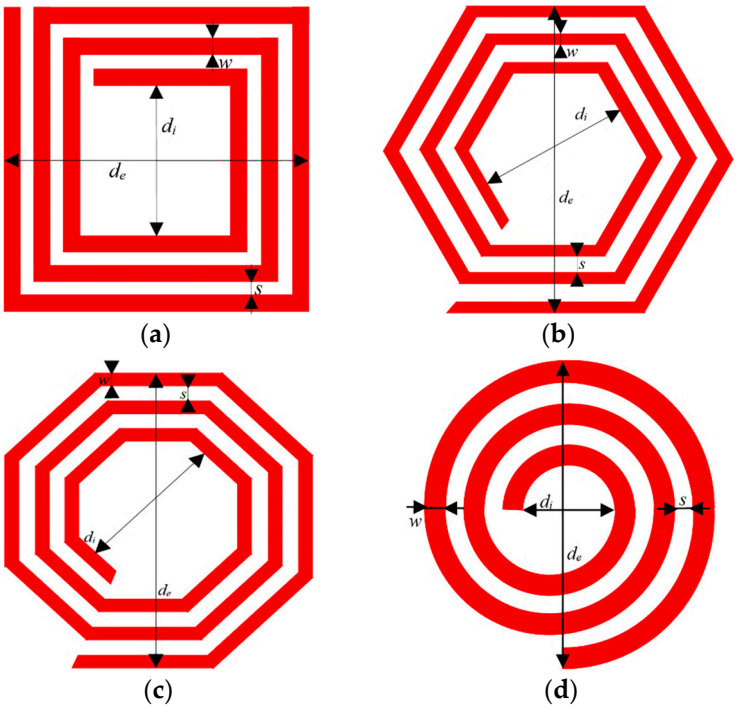


Figure 1. Geometric description of spiral planar inductors with (**a**) square; (**b**) hexagonal; (**c**) octagonal; and (**d**) circular shapes.

The following dependencies must be fulfilled between the descriptive geometric parameters, terms, and coefficients:

$$d_i \geq s, \tag{4}$$

$$d_e = d_i + 2Nw + 2(N-1)s, \tag{5}$$

$$d_e = d_{avg} + N(w+s) - s, \tag{6}$$

$$\rho = \frac{[n(w+s) - s]}{d_{avg}}, \tag{7}$$

where

- w is the turn width;
- s is the distance between adjacent turns;
- n is the number of layout sides;
- and C_1, C_2, C_3, and C_4 are geometrical constants according to the current sheet method [25] from Table 1.

Table 1. Coefficients for current sheet expression [25].

Layout	C_1	C_2	C_3	C_4
square	1.27	2.07	0.18	0.13
hexagonal	1.09	2.23	0.00	0.17
octagonal	1.07	2.29	0.00	0.19
circular	1.00	2.46	0.00	0.20

The authors have studied, analyzed, numerically modelled, optimally designed, and constructed these commonly used shapes designed on mono- or multilayer structures to

address applications across various domains [4,9,22,23,32]. A wide range of spiral inductors were initially designed, then modelled and finally constructed and measured to validate the analyses, formulas, and tools developed for extracting their parameters [9,22,23].

Figure 2 illustrates four planar spiral inductors with square, hexagonal, octagonal, and circular geometric shapes, which were analyzed, modelled, and constructed for exemplification. These inductors consist of 16 turns, with an outer diameter of 20 mm, a turn width of 0.4 mm, and a distance between the turns of 0.2 mm. The spirals are made of copper placed on an FR4 epoxy dielectric. The results obtained through analytical, numerical, and experimental approaches are summarized in Table 2. The analytical results were calculated using relation (1) and the geometrical coefficients listed in Table 1. Numerical results were extracted using two software programs; the first one is the ABSIF software (Version 1) program developed by authors. [23], and the second one is the commercial ANSYS-Q3D Extractor software (Version 2023 R1) package. The constructed inductors from Figure 2 were measured experimentally using a Precision LCR Bridge. Relative errors were calculated for each approach as follows: ε_{r1} (analytical vs. ABSIF); ε_{r2} (analytical vs. Q3D Extractor); and ε_{r3} (ABSIF vs. experimental measurements). Planar spiral inductors are extensively used in the design of various compact devices.

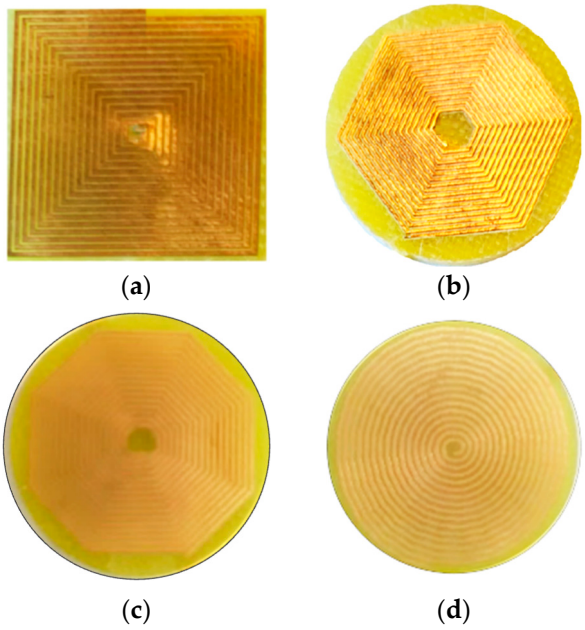


Figure 2. Constructed planar spiral inductors with the four conventional shapes: (**a**) square; (**b**) hexagonal; (**c**) octagonal; and (**d**) circular shapes.

Table 2. Results for the four shapes of planar spiral inductors that were obtained analytically, numerically, and experimentally.

Inductor Shape	Inductance, μH						
	Analytical	Numerical				Experimental Measurements	ε_{r3}
		ABSIF	ε_{r1}	Q3D Extractor	ε_{r2}		
Square	2.42	2.45	1.22	2.29	5.37	2.48	1.20
Hexagonal	2.52	2.63	4.36	2.48	1.58	2.91	9.62
Octagonal	2.29	2.36	3.05	2.11	7.86	2.52	6.34
Circular	2.05	2.01	1.95	2.02	1.46	2.12	5.18

The authors utilized these inductors to design and construct antennas, filters, and WPT systems, as well as RFID [4,9,32], though they are also employed in numerous other

high-tech applications [1–21,33,34]. Following extensive analysis and simulations, square and circular inductors were selected as the emitter and receiver, respectively, for our first prototype of WPT for a pacemaker, as presented in Figure 3. This prototype was initially tested with different types of lamps and the results were disseminated in the literature [9]. A solution was developed to enhance the performances of WPT by placing ferrite beneath the dielectric of the emitter inductor [32].

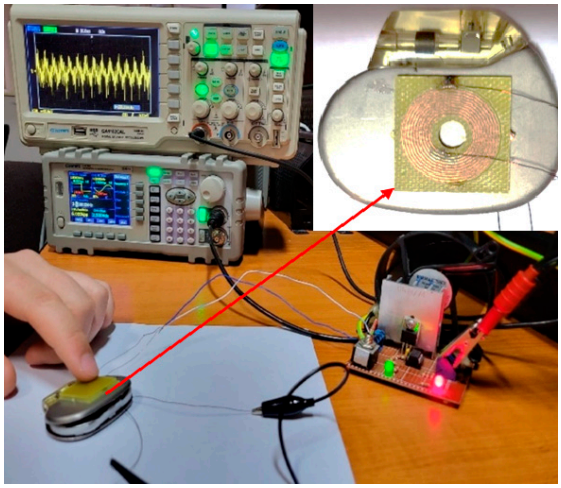


Figure 3. The wireless power transfer system prototype constructed of planar spiral inductors.

However, achieving high performances for the receiver inductor remains challenging, as ferrite cannot be used. To improve the power transfer efficiency of the WPT for pacemakers, it is essential to increase the inductance of inductors. Our proposed solution involves adapting the shape of the inductors to align with the pacemaker's shape. Selecting a shape for the copper spiral inductor that avoids ninety-degree angles offers a significant advantage. This design choice is expected to substantially increase the inductance, even when maintaining the same geometric parameters that influence inductance, such as the number of turns, turn width, and distance between turns.

3. Design of Oval Planar Spiral Inductor

Considering the shape of the pacemaker's external casing, we proposed a new inductor design that aligns perfectly with the device's form. As detailed in Figure 4, this design introduces an oval shape. Oval planar spiral inductors are ideal for use as both receivers and emitters in WPT systems for compact smart devices, offering enhanced compatibility and performance.

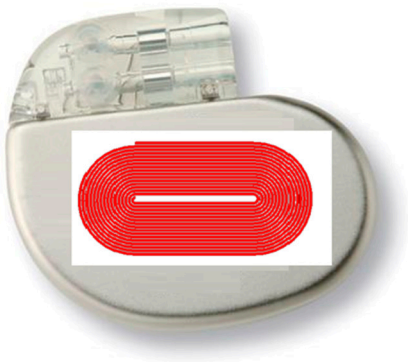


Figure 4. The oval planar spiral inductors for the WPT receiver and emitter.

3.1. Idea of the Oval Shape

A new shape has been designed to increase the inductance of the inductors. In the literature, we recently found the elliptical shape [16]. However, for our application, a wireless power transfer system to supply the pacemaker, none of the square, circular, octagonal, hexagonal, or elliptical shapes were suitable for optimally covering the shape of the pacemaker case. Therefore, we designed a new shape by starting by combining square and circular shapes (cut into two pieces) to form our oval shape presented in Figure 5, which matches our application perfectly.

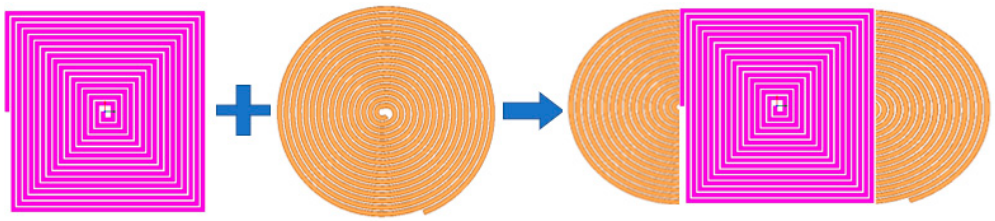


Figure 5. Design of planar spiral inductor with oval shape.

3.2. The Oval Planar Spiral Inductor

We designed the oval geometry to fit within an area of 40 × 20 mm^2, as presented in Figure 4. To compare and validate the new oval shape, we kept the same parameters as those used for the square, hexagonal, octagonal, and circular shapes that were designed, analyzed, modelled, and constructed, as mentioned in the second paragraph of this article: 16 turns, a turn width of 0.4 mm and a distance of 0.2 mm between turns, as shown in Figure 6. Additionally, the materials remain the same: copper for the inductor's spiral and FR4 epoxy for the dielectric substrate. Therefore, the number of turns, the distance between the turns, the turn width, and the materials are kept consistent with those used for the common shapes described in the previous sections. This allows for a comparison of the results with those for the standard shapes (Table 2) to determine whether the newly designed oval shape achieves an increase in inductance (L) and quality factor (Q).



Figure 6. The designed planar spiral inductor with an oval shape.

4. Numerical Modelling of Oval Planar Spiral Inductor

Before constructing our designed oval planar spiral inductor, we wanted to numerically model it to extract its inductance. We chose a commercial program software, ANSYS-Q3D Extractor, to carry this out. We drew the tridimensionality model of the oval spiral from copper, placed on an FR4 epoxy dielectric with the dimensions presented above. The implemented model of the planar oval spiral inductor is detailed in Figure 7; the spiral of copper with a red colour and the dielectric substrate with light yellow can be identified.

Figure 8 represents the current density in the oval spiral which confirms the constant field distribution all over the spiral inductor, succeeding with this shape to eliminate the non-uniformities that appear in the case of a square shape, as can be seen in Figure 9. The parameters extracted with the Q3D Extractor for this planar oval spiral inductor are presented in Table 3.

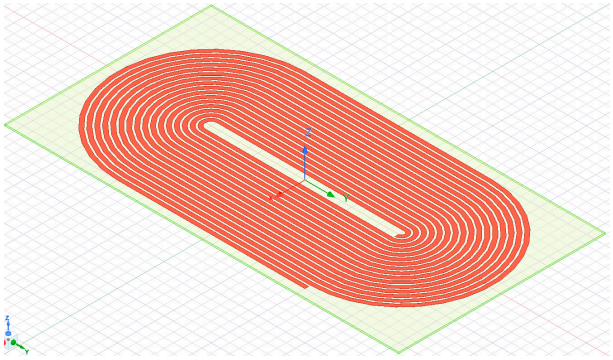


Figure 7. The modelled oval planar spiral inductor.

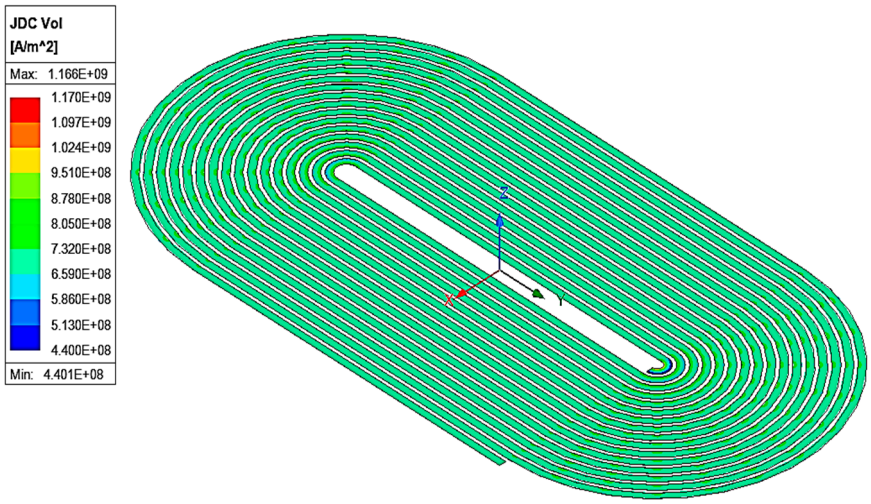


Figure 8. The current density distribution in the oval spiral inductor.

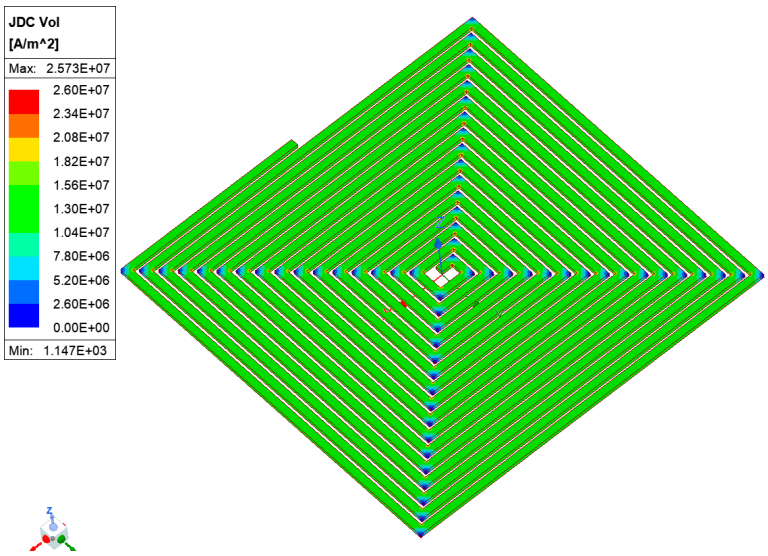


Figure 9. The current density distribution in the square spiral inductor.

Also, the square, hexagonal, octagonal, and circular spiral inductors were numerically modelled in the ANSYS-Q3D Extractor to compare the results. Figure 9 represents the exemplification and comparison of the current density only for the square spiral inductor, noting that it is not uniformly distributed. Table 4 shows the extracted parameters for it. Unexpectedly, we were able to significantly increase the inductance; therefore, by

comparing the simulation results for the square and oval shapes, we observed a 2.27 times increase in inductance.

Table 3. Modelled oval planar spiral inductor parameters.

Parameter	Oval Planar Spiral Inductor	
	dc	ac
Inductance, μH	5.229	5.132
Resistance, Ω	14.272	195.44
Capacitance, pF	1.022	

Table 4. Modelled planar square spiral inductor parameters.

Parameter	Planar Square Spiral Inductor	
	dc	ac
Inductance, μH	2.296	2.126
Resistance, Ω	0.141	22.447
Capacitance, pF	0.874	

We achieved this significant increase in inductance for the oval spiral inductor due to the following factors: the maximum number of turns considered, 16 turns, that perfectly fit into the available area; the increased enclosed area of the spiral; the strong magnetic flux coupling between tightly packed turns, with a distance of 0.2 mm between them; the reduced magnetic field leakage; the elimination of ninety-degree angles in the inductor's layout; and the larger effective length of the spiral.

5. Construction of Oval Planar Spiral Inductor for Shape Validation

To ensure that the inductance obtained by numerical modelling is correct, we constructed the planar oval spiral inductor and measured its inductance. In this way, we can be confident that the new shape that we propose can be an ideal one for many applications. Planar oval spiral inductor construction uses the LPKF PCB production line, more precisely LPKF ProtoMat S103, LPKF Laser&Electronisc SE, Garbsen, Germany, we bought from the local distributor, Interbusiness Promotion & Consulting S.R.L., ISO Certificate 9001:2015, 023594-Bucharest, Romania, as presented in Figure 10. We imported the oval planar spiral inductor geometry from the Q3D Extractor to the LPKF Circuit Pro software (Version PM 2.3) program to construct it.



Figure 10. Equipment used to construct planar spiral inductors.

Figure 11 presents the constructed oval planar spiral inductor with a size of 20 × 40 mm size, with 16 turns, a turn width of w = 0.4 mm, and a distance between the turns of s = 0.2 mm, the same as the numerically modelled configuration.

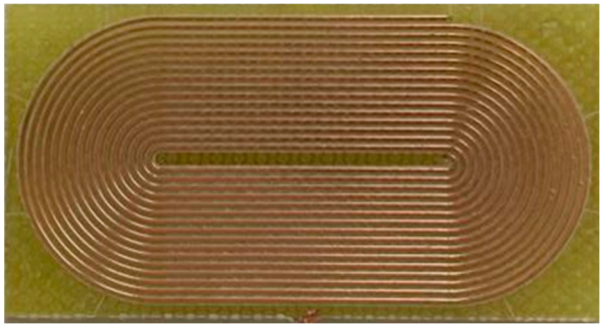


Figure 11. Constructed oval planar spiral inductor.

Once the oval planar spiral inductor is constructed, we can measure its inductance using a Precision LCR Bridge to ensure that the inductance of the new oval shape is greater than that of square, hexagonal, octagonal, and circular shapes. The inductance measured for the oval spiral inductor with the LCR Meter is 5.36 µH, as shown in Figure 12.

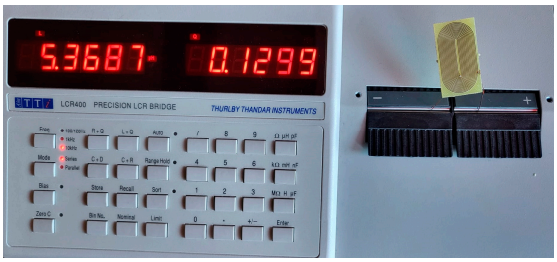
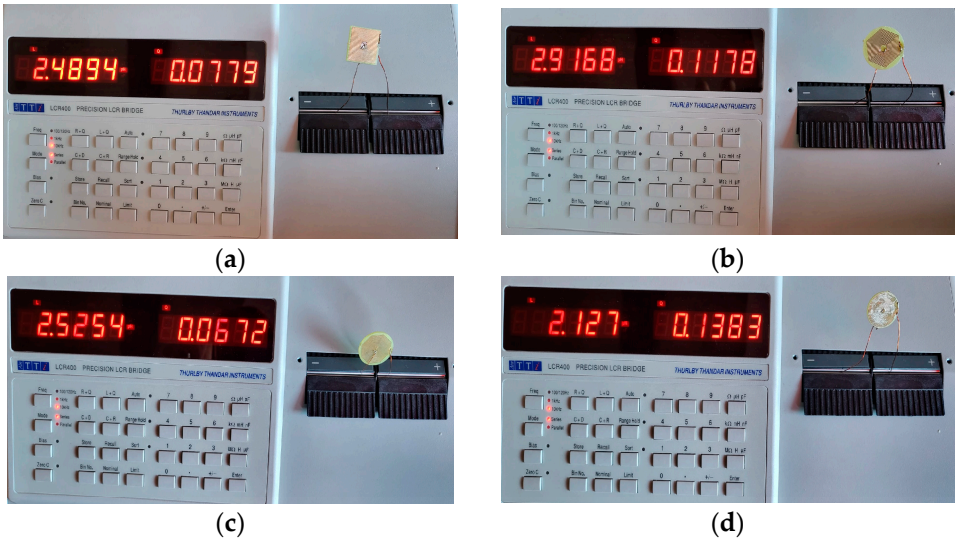


Figure 12. The inductance measured for the constructed oval planar spiral inductor.

The experimental measurements performed with the same LCR Meter for square, hexagonal, octagonal, and circular spiral inductors with 16 turns and identical dimensions for the geometrical parameters, all constructed with the same LPKF ProtoMat 103, are presented in Figure 13. The experimental results show that the oval inductor exhibits an inductance 2.16 times greater than the square shape, 1.84 times greater than the hexagonal shape, 2.12 times greater than the octagonal shape, and 2.52 times greater than the circular shape, as detailed in Table 5. Now, we are convinced that using the new oval shape results in a higher inductance. The quality factor is also increased, as can be verified from the experimental measurements in Figures 12 and 13 and Table 5.

By designing this new oval shape, several key advantages can be mentioned: uniform current distribution (this minimizes hotspots and ensures better performance under high-frequency conditions); higher quality factor (fewer sharp edges and corners reduce losses due to current crowding); lower parasitic effects (a more symmetric structure reduces parasitic capacitances and inductance variation, with this being particularly advantageous in high-frequency and RF applications); improved magnetic field distribution (the magnetic field is more evenly distributed and this reduces interference with surrounding components and enhances overall efficiency); mechanical stability (better mechanical strength and durability due to their continuous structure without sharp angles, making them less prone to deformation under stress or thermal expansion); aesthetic and compact design (these are easier to integrate into rounded enclosures); and last but not least, the most important one, increased inductance. We conclude that it is better to choose oval shapes over traditional ones for high-frequency applications, where the Q factor and reduced parasitic effects

are critical, for compact designs requiring efficient use of space and minimal interference and for thermal reliability where uniform current distribution is important. However, square inductors might still be preferred in certain applications due to ease of fabrication, better utilization of PCB space, or alignment with other components. The choice ultimately depends on the specific requirements of the circuit and the manufacturing process.



(**a**) (**b**) (**c**) (**d**)

Figure 13. The inductance measured for the constructed planar spiral inductor with the following shapes: (**a**) square, (**b**) hexagonal, (**c**) octagonal, and (**d**) circular.

Table 5. Experimental results for inductance and quality factor.

Inductor Shape	Experimental Measurement Results	
	Inductance, μH	Quality Factor
Oval	5.3685	0.129
Square	2.489	0.077
Hexagonal	2.916	0.117
Octagonal	2.525	0.067
Circular	2.127	0.138

The oval shape spiral inductor generally exhibits differences in parasitic resistance (R), parasitic capacitance (C), and quality factor (Q) when compared to circular or square inductors, primarily due to its unique geometry. The oval shape inductor may have a higher parasitic resistance compared to circular inductors due to the less efficient current flow in regions with tighter curvatures. However, this increase in resistance may be less pronounced than in square inductors, where sharp corners can cause higher resistance due to increased current density at the corners. Parasitic capacitance in the oval inductor is typically lower than in a square inductor due to the smoother curves and more gradual changes in the geometry, which reduce the chances of significant electric field buildup. In comparison, the corners of a square inductor often contribute to higher capacitance due to the sharp edges and increased proximity of conductors. The oval shape, with its continuous curvature, usually leads to a more uniform electric field distribution, reducing capacitance. The quality factor (Q) of an oval shape inductor is generally higher than that of a square inductor because of the reduced parasitic capacitance and less resistance due to the smoother geometry. The circular inductor, with its symmetrical structure, may also have a high Q factor, potentially higher than the oval inductor depending on the design parameters. However, oval inductors may still perform better in certain designs where size or inductance value optimizations are crucial. In summary, oval shape inductors can offer

advantages in terms of lower parasitic capacitance and potentially higher quality factors compared to square inductors, while the parasitic resistance may be slightly higher than that of circular inductors due to the less optimal current path in regions with tight curvatures.

6. Adapting the Inductance Formula for the Oval Spiral Inductor

Based on the inductance formula for the four common shapes of planar spiral inductors, as shown in expression (1), we want to use it to calculate the inductance for the new oval shape that was designed, modelled, and constructed. Due to the non-symmetry of geometry, more concepts are needed. The oval shape is semi-symmetrical, so some of the descriptive parameters from relation (1), such as the fill ratio and the average diameter, must be adapted, and new relations such as (8)–(11) are developed. Figure 14 provides a description of the geometric parameters that characterize the oval planar spiral shape (number of turns, N; turn width, w; distance between turns, s; outer diameters, D_o and d_o; and inner diameters, D_i and d_i). Analogous to the current sheet method [25] and the relations from [16], we need the average diameter and the fill ratio, which, here, for this semi-symmetrical geometry, are different.

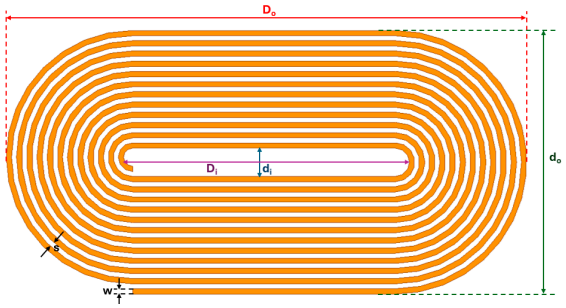


Figure 14. Descriptive parameters of the oval spiral inductor.

Analyzing the geometry, we identify four diameters that describe the structure; therefore, the two outer diameters are as follows:

- D_o is the outer diameter along the length of the oval inductor's plane;
- d_o is the outer diameter along the width of the oval inductor's plane.
- And the two inner diameters are as follows:
- D_i is the inner diameter along the length of the oval inductor's plane;
- d_i is the inner diameter along the width of the oval inductor's plane.

From a geometric point of view, we define an outer diameter as a geometric mean:

$$D_{out} = \sqrt{D_o \cdot d_o}, \tag{8}$$

and similarly, we define an inner diameter as follows:

$$D_{int} = \sqrt{D_i \cdot d_i}, \tag{9}$$

Using these geometric means for the outer and inner diameters, we adapted the average diameter for the oval shape, which can be determined using the following adapted relation:

$$d_{avg_oval} = \frac{D_{out} + D_{\text{int}}}{2}, \tag{10}$$

and similarly, the fill factor, ρ_{oval}, can be calculated with the adapted relation:

$$\rho_{oval} = \frac{D_{out} - D_{\text{int}}}{D_{out} + D_{\text{int}}}, \tag{11}$$

Therefore, the inductance of the oval spiral inductor can be calculated using the formula for common shapes, where the average diameter and the fill ratio have been determined using relations (10) and (11):

$$L_{oval} = \frac{\mu N^2 d_{avg_oval} C_1}{2}\left[\ln\left(\frac{C_2}{\rho_{oval}}\right) + C_3\rho_{oval} + C_4{\rho_{oval}}^2\right]. \quad (12)$$

If we consider the coefficients C_1, C_2, C_3, and C_4 (Table 1) to be those for the circular shape, as was similarly carried out for the elliptical shape in [16], we obtain an inductance of 3.64 µH, which is incorrect compared to experimental and numerical modelling results for the oval inductor described above. Additionally, if we calculate the inductance of the square and circular inductors separately and add them, we still obtain an incorrect value of 4.47 µH (Table 2) because, for the oval shape, the numerical inductance obtained is 6.22 µH, and the experimental value is 6.36 µH. The average diameter and the fill ratio are correctly expressed by relations (10) and (11); therefore, the coefficients cannot be the same as those for the circular shape (Table 1) as is considered for the elliptical shape in [16]. New C_1, C_2, C_3, and C_4 coefficients are required for the new oval shape, and we determined them using the current sheet method, as well as mathematical algorithms and tools.

7. Numerical and Experimental Coefficient Determination and Inductance Expression Validation for Oval Planar Spiral Inductors

Five sets of spiral inductors with oval shapes were designed, numerically modelled, and constructed to determine the appropriate coefficients and validate the new formula (12). Various dimensions for the geometric parameters and different numbers of turns were considered to cover a wide range of oval spiral configurations, ensuring the accuracy of our results.

7.1. Numerical Modelling of Oval Spiral Inductors

We modelled them using the software program ANSYS-Q3D Extractor to extract the inductance for each inductor. The first set of oval spiral inductors was designed with smaller dimensions, and in Figure 15, four structures are presented as examples, showing their real size. The outer diameters are the same for all the inductors in this set: D_o = 20 mm and d_o = 10 mm. The number of turns is variable between 2 and 16 turns; the width of the turn, w, is between 0.2 and 0.3 mm; and the distance between the turns, s, varies from 0.1 to 0.25 mm. In Table 6, the extracted parameters for the four oval inductors from the first set are synthesized for exemplification.

The second set of the oval spiral inductors is presented in Figure 16. The dimensions for the outer diameters are D_o = 30 mm and d_o = 15 mm, the number of turns range from 1 to 15; the turn width, w, is between 0.25 and 0.5 mm; and the distance between turns, s, ranges from 0.2 to 0.5 mm.

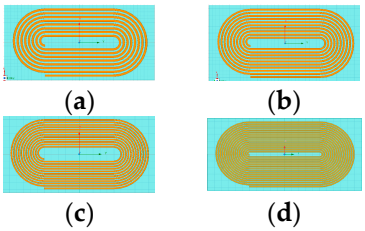


Figure 15. First set of oval spiral inductors designed and numerically modelled with 10 × 20 mm dimensions: (**a**) 8 turns, w = 0.3 mm, s = 0.25 mm; (**b**) 10 turns, w = 0.25 mm, s = 0.2 mm; (**c**) 12 turns, w = 0.2 mm, s = 0.15 mm; and (**d**) 16 turns, w = 0.2 mm, s = 0.1 mm.

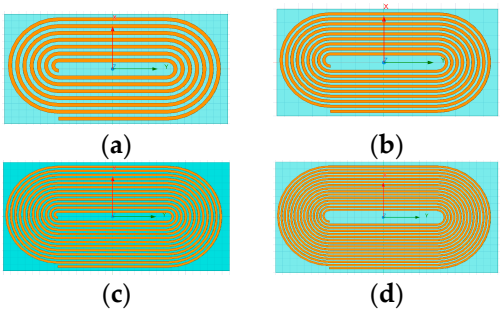


Figure 16. Second set of oval spiral inductors designed and numerically modelled with 15 × 30 mm dimensions: (**a**) 7 turns, w = 0.5 mm, s = 0.5 mm; (**b**) 9 turns, w = 0.4 mm, s = 0.35 mm; (**c**) 12 turns, w = 0.3 mm, s = 0.3 mm; and (**d**) 15 turns, w = 0.25 mm, s = 0.2 mm.

Table 6. Numerical results for 1st set of oval inductors.

Number of Turns	**8**		**10**		**12**		**16**	
Results	**dc**	**ac**	**dc**	**ac**	**dc**	**ac**	**dc**	**ac**
Resistance [Ω]	4.93	0.09	7.34	0.13	11.29	0.17	14.27	0.32
Inductance [μH]	0.77	0.76	1.16	1.14	1.82	1.79	2.61	2.56
Capacitance [pF]	0.60		0.59		0.59		0.53	

Table 7 shows the extracted parameters for the four oval inductors from the second set, detailed for exemplification.

Table 7. Numerical results for 2nd set of oval inductors.

Number of Turns	**7**		**9**		**12**		**15**	
Results	**dc**	**ac**	**dc**	**ac**	**dc**	**ac**	**dc**	**ac**
Resistance [Ω]	3.8	0.09	6.19	0.14	10.75	0.02	16.53	0.28
Inductance [μH]	0.83	0.81	1.42	1.39	2.22	2.23	3.87	3.81
Capacitance [pF]	0.88		0.86		0.93		0.89	

Starting from the first oval spiral inductor (Figure 6) designed, modelled and constructed, we created the third set (Figure 17), keeping the same outer diameters, Do and do, while varying the number of turns from 1 to 16; the turn width, w, between 0.4 and 0.8 mm; and the distance between turns, s, from 0.2 to 0.3 mm.In Figure 17, four inductors from the third set are presented for exemplification. In Table 8, the extracted parameters for the four oval inductors from the third set are summarized for illustration purposes.

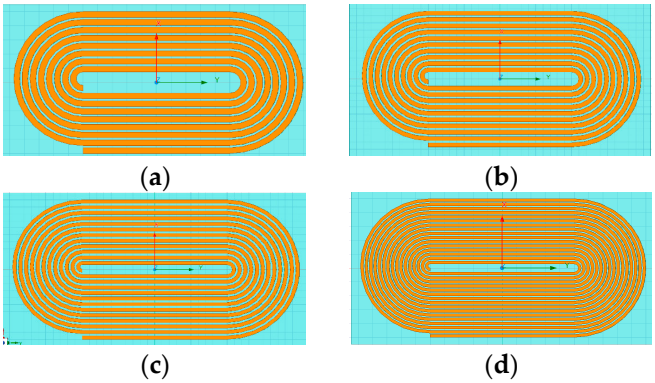


Figure 17. Third set of oval spiral inductors designed and numerically modelled with 20 × 40 mm outer diameters: (**a**) 8 turns, w = 0.8 mm, s = 0.3 mm; (**b**) 10 turns, w = 0.6 mm, s = 0.3 mm; (**c**) 12 turns, w = 0.5 mm, s = 0.3 mm; and (**d**) 16 turns, w = 0.4 mm, s = 0.2 mm.

Table 8. Numerical results for 3rd set of oval inductors.

Number of Turns	**8**		**10**		**12**		**16**	
Results	**dc**	**ac**	**dc**	**ac**	**dc**	**ac**	**dc**	**ac**
Resistance [Ω]	3.66	0.19	5.93	0.25	8.56	0.29	14.27	0.05
Inductance [μH]	1.49	1.45	2.24	2.19	2.97	2.91	5.23	5.13
Capacitance [pF]	1.10		1.10		1.14		1.16	

The fourth set of the oval spiral inductors is presented in Figure 18. Large outer diameters, D_o = 60 mm and d_o = 30 mm, are considered, with the number of turns ranging from 1 to 15; turn widths, w, between 0.5 and 1.1 mm; and distances between turns, s, from 0.4 to 0.8 mm.

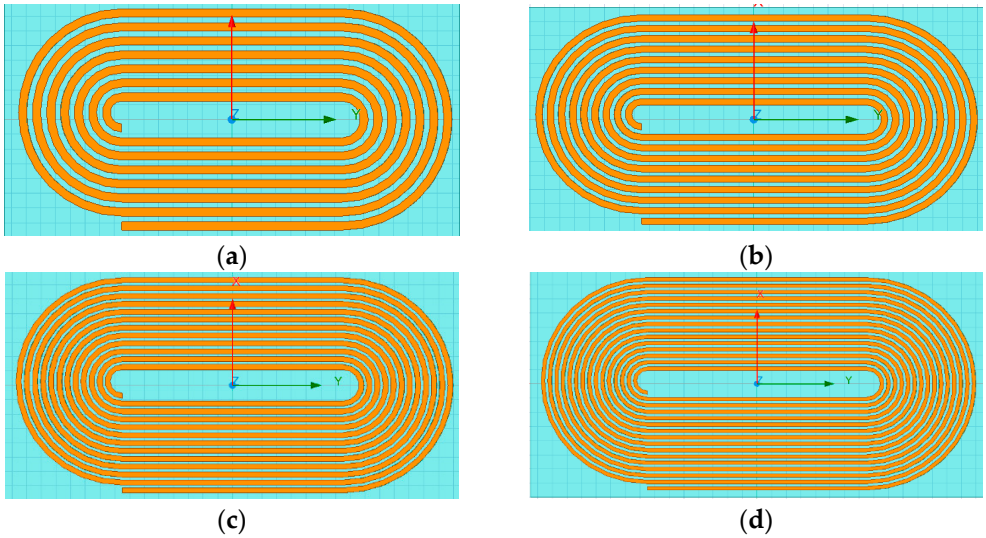


Figure 18. Fourth set of oval spiral inductors designed and numerically modelled with 30 × 60 mm dimensions: (**a**) 7 turns, w = 1.1 mm, s = 0.8 mm; (**b**) 9 turns, w = 0.9 mm, s = 0.6 mm; (**c**) 12 turns, w = 0.7 mm, s = 0.4 mm; and (**d**) 15 turns, w = 0.5 mm, s = 0.4 mm.

Table 9 summarizes the extracted parameters for the four oval inductors from the fourth set, provided for exemplification.

Table 9. Numerical results for 4th set of oval inductors.

Number of Turns	**7**		**9**		**12**		**15**	
Results	**dc**	**ac**	**dc**	**ac**	**dc**	**ac**	**dc**	**ac**
Resistance [Ω]	3.51	0.16	5.49	0.23	9.49	0.36	16.53	1.23
Inductance [μH]	1.76	1.72	2.80	2.75	5.09	4.99	7.74	7.65
Capacitance [pF]	1.72		1.70		1.65		1.71	

The fifth set of the oval spiral inductors is presented in Figure 19. The big dimensions were considered here, with outer diameters, D_o = 80 mm and d_o = 40 mm; turn widths, w, between 0.8 and 1.4 mm; and distances between turns, s, from 0.4 to 0.9 mm. Table 10 presents the extracted parameters for the four oval inductors from the fifth set.

Table 10. Numerical results for 5th set of oval inductors.

Number of Turns	8		10		12		16	
Results	**dc**	**ac**	**dc**	**ac**	**dc**	**ac**	**dc**	**ac**
Resistance [Ω]	4.14	0.25	6.09	0.36	10.89	0.38	14.69	0.79
Inductance [μH]	2.86	2.80	4.55	4.46	6.37	6.28	10.46	10.29
Capacitance [pF]	2.18		2.21		2.29		2.21	

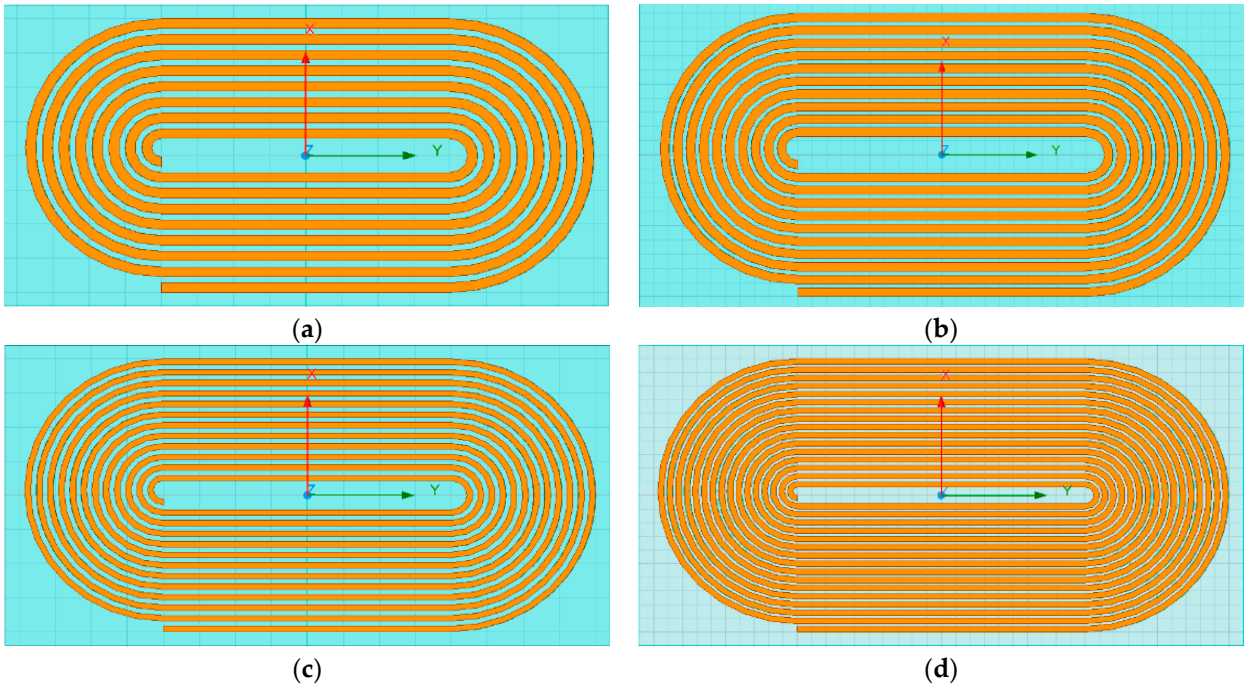
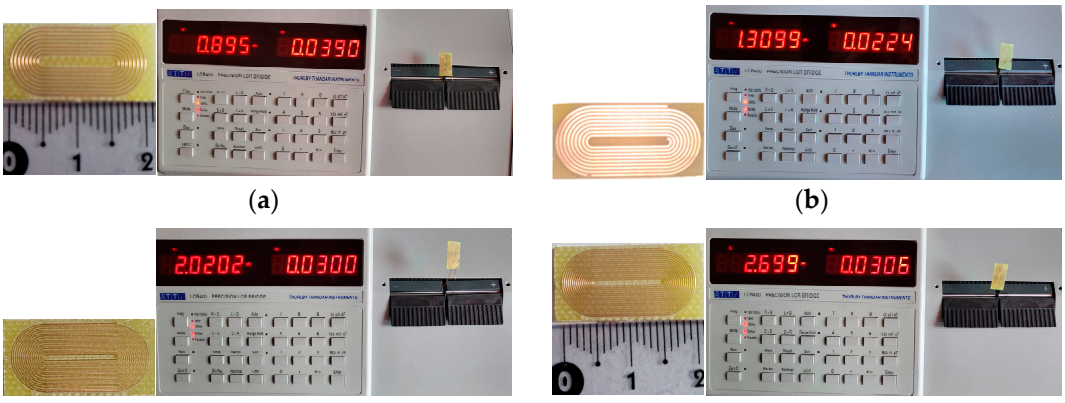


Figure 19. Fifth set of oval spiral inductors designed and numerically modelled with 40 × 80 mm dimensions: (**a**) 8 turns, w = 1.4 mm, s = 0.9 mm; (**b**) 10 turns, w = 1.2 mm, s = 0.6 mm; (**c**) 12 turns, w = 0.8 mm, s = 0.75 mm; and (**d**) 16 turns, w = 0.8 mm, s = 0.4 mm.

7.2. Construction of Oval Spiral Inductors for Experimental Validation

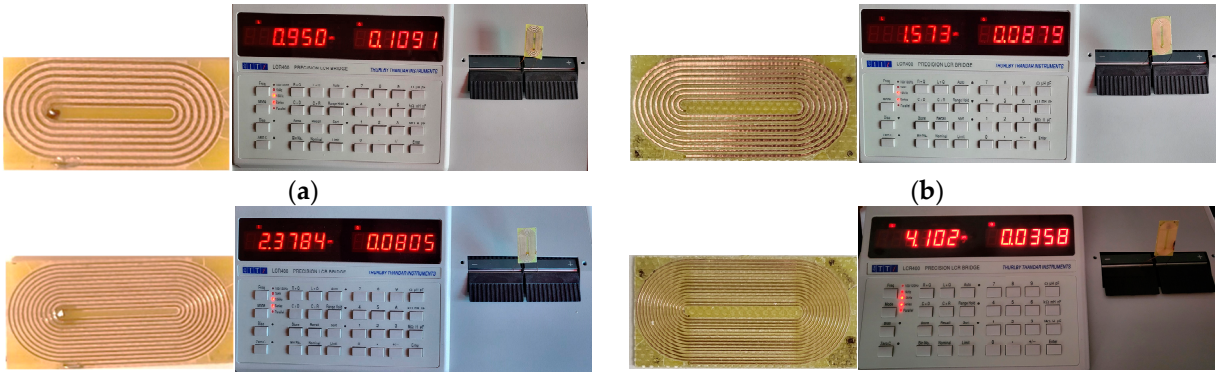
In accordance with the good results obtained through numerical modelling, the five sets of the designed oval planar spiral inductors were practically constructed using LPKF ProtoMat S103 to measure their inductances, desiring an experimental validation of the newly designed shape. Figures 20–24 detail the inductance measurements for the wide range of designed sets of spiral inductors with oval shapes.

The results obtained through numerical modelling using the Q3D Extractor tool from the ANSYS software package are compared with the experimental measurements performed using the Aim-TTi LCR400 Bench LCR Meter, AIM & THURLBY THANDAR INSTRUMENTS, Huntingdon, England, we bought them from the local distributor SC Comtest SRL, Timisoara, Romania, as summarized in Table 11. The relative errors range from 2.12% to 13.63%. By analyzing the dimensions of the sets of spiral inductors, it can be observed that a wide range of layouts were designed, numerically modelled, and constructed to successfully validate this new shape. All the obtained results are consistent and provide the foundation for the next step: determining the new coefficients for the proposed shape of the planar spiral inductor.



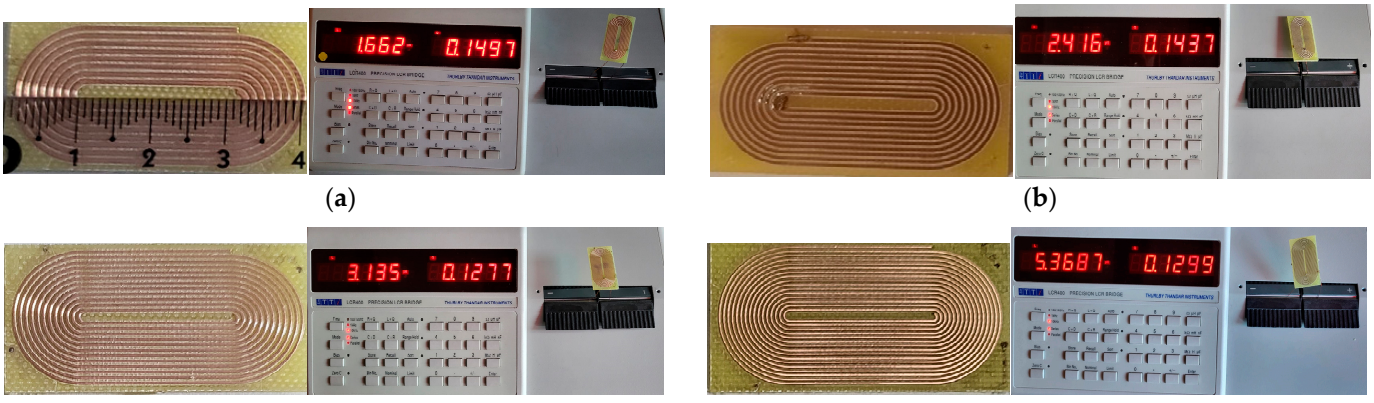
(**a**) (**b**) (**c**) (**d**)

Figure 20. First set (10 × 20 mm) of constructed oval inductors: (**a**) 8 turns, w = 0.3 mm, s = 0.25 mm; L = 0.895 μH and quality factor, Q = 0.039; (**b**) 10 turns, w = 0.25 mm, s = 0.2 mm; L = 1.30 μH and Q = 0.0224; (**c**) 12 turns, w = 0.2 mm, s = 0.15 mm; L = 2.02 μH and Q = 0.03; and (**d**) 16 turns, w = 0.2 mm, s = 0.1 mm; L = 2.69 μH and Q = 0.03.



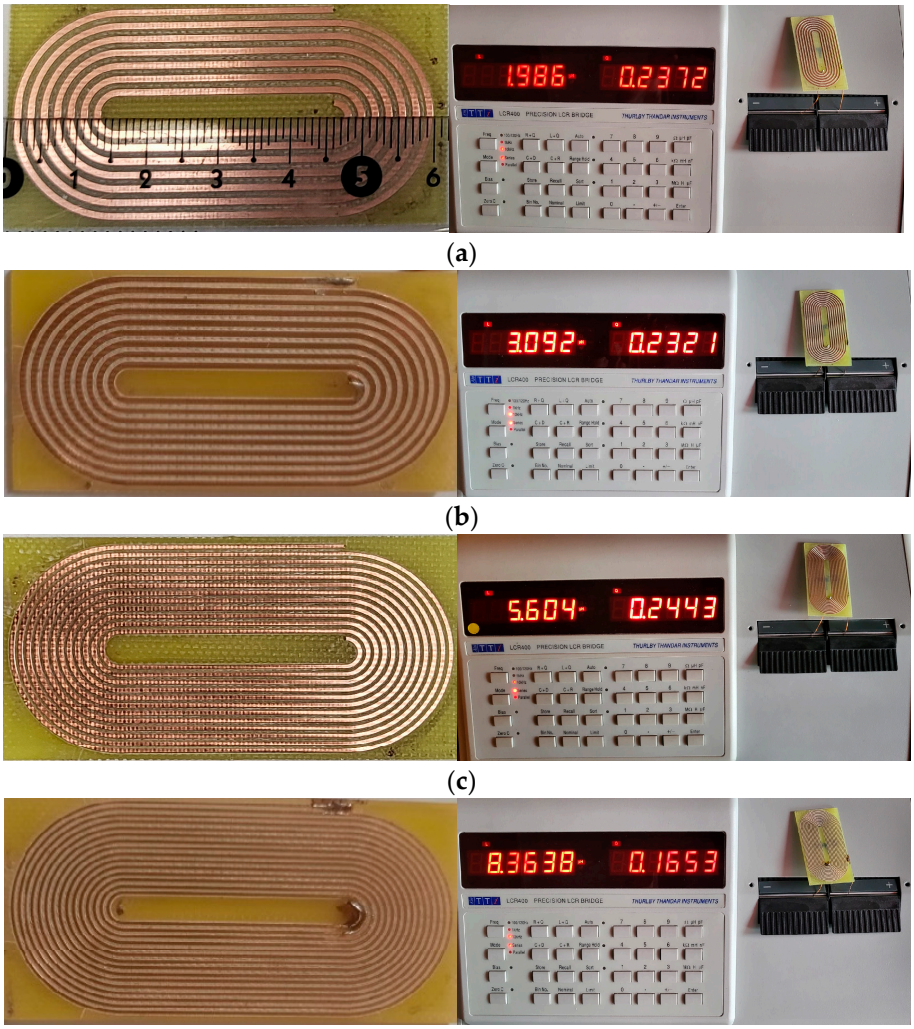
(**a**) (**b**) (**c**) (**d**)

Figure 21. Second set (15 × 30 mm) of constructed oval inductors: (**a**) 7 turns, w = 0.5 mm, s = 0.5 mm; L = 0.95 μH and quality factor, Q = 0.109; (**b**) 9 turns, w = 0.4 mm, s = 0.35 mm; L = 1.57 μH and Q = 0.087; (**c**) 12 turns, w = 0.3 mm, s = 0.3 mm; L = 2.37 μH and Q = 0.08; and (**d**) 15 turns, w = 0.25 mm, s = 0.1 mm; L = 4.10 μH and Q = 0.035.



(**a**) (**b**) (**c**) (**d**)

Figure 22. Third set (20 × 40 mm) of constructed oval inductors: (**a**) 8 turns, w = 0.8 mm, s = 0.3 mm; L = 1.662 μH and Q = 0.149; (**b**) 10 turns, w = 0.6 mm, s = 0.3 mm; L = 2.416 μH and Q = 0.143; (**c**) 12 turns, w = 0.5 mm, s = 0.3 mm; L = 3.135 μH and Q = 0.127; and (**d**) 16 turns, w = 0.4 mm, s = 0.2 mm; L = 5.368 μH and Q = 0.129.



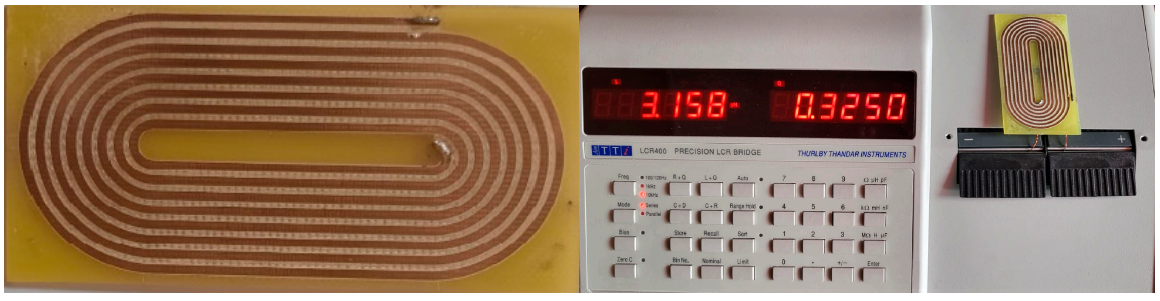
(**a**)

(**b**)

(**c**)

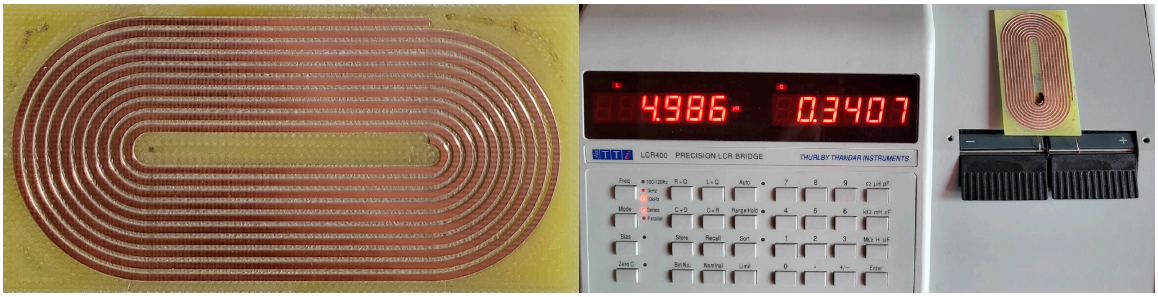
(**d**)

Figure 23. Fourth set (30 × 60 mm) of constructed oval inductors: (**a**) 7 turns, w = 1.1 mm, s = 0.8 mm; L = 1.986 μH and Q = 0.237; (**b**) 9 turns, w = 0.9 mm, s = 0.6 mm; L = 3.092 μH and Q = 0.232; (**c**) 12 turns, w = 0.7 mm, s = 0.4 mm; L = 5.604 μH and Q = 0.244; and (**d**) 15 turns, w = 0.5 mm, s = 0.4 mm; L = 8.363 μH and Q = 0.165.



(**a**)

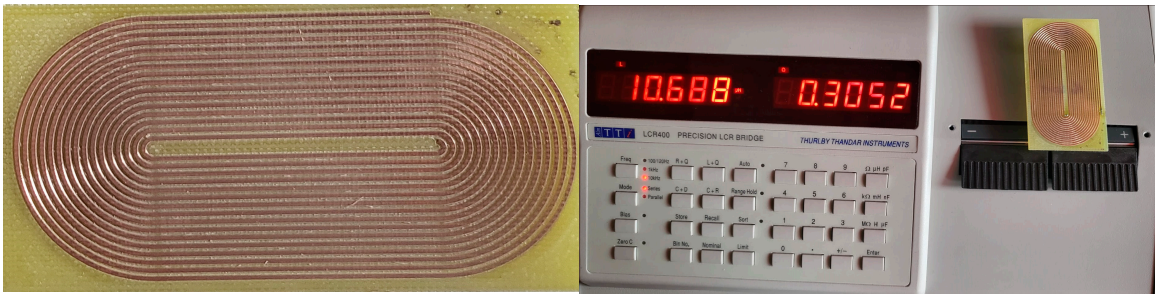
Figure 24. *Cont.*



(**b**)



(**c**)



(**d**)

Figure 24. Fifth set (40 × 80 mm) of constructed oval inductors: (**a**) 8 turns, w = 1.4 mm, s = 0.9 mm; L = 3.158 μH and Q = 0.325; (**b**) 10 turns, w = 1.2 mm, s = 0.6 mm; L = 4.986 μH and Q = 0.340; (**c**) 12 turns, w = 0.8 mm, s = 0.75 mm; L = 6.805 μH and Q = 0.241; and (**d**) 16 turns, w = 0.8 mm, s = 0.4 mm; L = 10.688 μH and Q = 0.305.

Table 11. Comparison of the results: numerical modelling vs. experimental results for the five sets of oval spiral inductors designed.

Set of Inductors	N, turns	D_o, mm	d_o, mm	w, mm	s, mm	Q3D Extractor, μH	L Measured, μH	Error, %
1st	8	20	10	0.3	0.25	0.773	0.895	13.63
	10	20	10	0.25	0.2	1.159	1.309	11.45
	12	20	10	0.2	0.15	1.820	2.020	9.90
	16	20	10	0.2	0.1	2.610	2.699	3.29
2nd	7	30	15	0.5	0.5	0.833	0.950	12.31
	9	30	15	0.4	0.35	1.421	1.573	9.66
	12	30	15	0.3	0.3	2.227	2.378	6.34
	15	30	15	0.25	0.2	3.870	4.102	5.65
3rd	8	40	20	0.8	0.3	1.492	1.662	10.22
	10	40	20	0.6	0.3	2.249	2.416	6.91
	12	40	20	0.5	0.3	2.973	3.135	5.16
	16	40	20	0.4	0.2	5.229	5.368	2.58
4th	7	60	30	1.1	0.8	1.756	1.986	11.58
	9	60	30	0.9	0.6	2.805	3.092	9.28
	12	60	30	0.7	0.4	5.088	5.604	9.20
	15	60	30	0.5	0.4	7.741	8.363	7.43
5th	8	80	40	1.4	0.9	2.864	3.158	9,30
	10	80	40	1.2	0.6	4.553	4.986	8.68
	12	80	40	0.8	0.75	6.369	6.805	6.40
	16	80	40	0.8	0.4	10.461	10.688	2.12

7.3. Determination of the Coefficients for Oval Shape

The inductance of the new oval spiral inductor will be analytically determined using the newly developed relation (12). In this relation, new coefficients, C_1, C_2, C_3, and C_4, are required, as the coefficients for the circular shape from Table 1 are not applicable to the oval shape (see Section 6).

By analyzing the analytical results obtained through the implementation of relation (12) in mathematical tools and the numerical and experimental results, for a wide range of oval spiral inductors designed by authors, and based on the current sheet method, similar to [25], the coefficients for the oval shape are determined to be $C_1 = 1.39$, $C_2 = 2.48$, $C_3 = 0$, and $C_4 = 0.2$. Relation (12) was applied to the five sets of designed, numerically modelled, and constructed oval inductors to obtain the inductance using an analytical approach. The following variation in parameters was considered: $N = 1 \div 16$ turns; $w = 0.1 \div 1.5$ mm; $s = 0.1 \div 1$ mm; and the outer diameters described above for each of the sets. The inductances for more than four hundred oval inductors were analytically determined. Using mathematical algorithms, these new coefficients were selected to be the ones that provide the minimal errors in relation to the experimental measurements. Next, these new coefficients are validated both experimentally and numerically.

7.4. Inductance Formula and Coefficients Experimental Validation

To validate the coefficients and the formula for inductance computation, they must be verified. Validation is carried out through both experimental and numerical approaches. The inductance Formula (12) is used to calculate the values for each of the five sets of oval spiral inductors that were designed. First, the results are compared with those experimentally measured using the LCR 400 Precision LCR Bridge, as detailed in Section 7.2. For comparison, the results from the analytical and experimental approaches for the five sets of oval spiral inductors designed are summarized in Table 12.

Table 12. Experimental validation of the inductance formula and coefficients for the oval shape: A comparison between analytical and experimental results for the five sets of designed oval spiral inductors.

Set of Inductors	N, turns	D_o, mm	d_o, mm	w, mm	s, mm	L Formula (12), µH	L Measured, µH	Error, %
1st	8	20	10	0.3	0.25	0.839	0.895	6.25
	10	20	10	0.25	0.2	1.229	1.309	6.11
	12	20	10	0.2	0.15	1.969	2.020	2.52
	16	20	10	0.2	0.1	2.545	2.699	5.70
2nd	7	30	15	0.5	0.5	0.895	0.950	5.78
	9	30	15	0.4	0.35	1.516	1.573	3.62
	12	30	15	0.3	0.3	2.282	2.378	4.03
	15	30	15	0.25	0.2	4.021	4.102	1.97
3rd	8	40	20	0.8	0.3	1.609	1.662	3.18
	10	40	20	0.6	0.3	2.402	2.416	0.57
	12	40	20	0.5	0.3	2.954	3.135	5.77
	16	40	20	0.4	0.2	5.089	5.368	5.19
4th	7	60	30	1.1	0.8	1.915	1.986	3.57
	9	60	30	0.9	0.6	2.986	3.092	3.42
	12	60	30	0.7	0.4	5.389	5.604	3.83
	15	60	30	0.5	0.4	8.043	8.363	3.82
5th	8	80	40	1.4	0.9	3.038	3.158	3.79
	10	80	40	1.2	0.6	4.804	4.986	3.65
	12	80	40	0.8	0.75	6.550	6.805	3.74
	16	80	40	0.8	0.4	10.180	10.688	4.75

Next, the results are compared with those numerically obtained using the Q3D Extractor tool for extracting the inductance by implementing each inductor layout into the tool separately which requires a long time and computational resources. After analyzing

the error between the analytical results, obtained using relation (12), and the experimental measurements taken with the LCR Meter, the very small errors, ranging from 0.57% to 6.25%, highlight the accuracy of our results.

These findings confirm the accuracy and reliability of the adapted formula, as well as the appropriateness of the geometric coefficients applied specifically to the design and analysis of oval spiral inductors. Experimental validation ensures that the formula produces results that align with real-world observations, confirming its precision and reliability. Validating a formula experimentally boosts confidence among researchers and practitioners by demonstrating its practical applicability. Experimental validation creates a foundation for further research and development, paving the way for innovations and advanced applications. Based on these findings, we can add another row to Table 1 [25], which is now updated as Table 13.

Table 13. Coefficients for oval layout/shape of spiral planar inductor.

Layout/Shape of Inductor	C_1	C_2	C_3	C_4
square [25]	1.27	2.07	0.18	0.13
hexagonal [25]	1.09	2.23	0.00	0.17
octagonal [25]	1.07	2.29	0.00	0.19
circular [25]	1.00	2.46	0.00	0.20
elliptical [16]	1.00	2.46	0.00	0.20
oval	1.39	2.48	0.00	0.20

7.5. Inductance Formula and Coefficients Analytical Validation

The inductance Formula (12) is used to calculate the values for each of the five sets of designed oval spiral inductors. Table 14 presents the analytical results compared with the numerical results obtained using ANSYS-Q3D Extractor, along with the relative error percentages for four configurations from each of the five sets of oval planar spiral inductors. The oval spiral inductors were made on the same dielectric material, FR4 epoxy, with a thickness of 1.51 mm and a relative permittivity of 4.4. The spiral is made of copper, which has a thickness of 35 µm, a relative permittivity of 0.999991, and a bulk conductivity of 5.8×10^7 S/m. The frequency considered for both measurements and simulations is 10 kHz. After analyzing the relative errors obtained from the analytical and numerical results, which range from 0.64% and 9.05%, it is again demonstrated that the new oval shape, the new inductance computation formula, and the new coefficients are validated. Analytical validation confirms that all of these produce results that are accurate and reliable for their intended purpose.

Table 14. Analytical vs. numerical inductance results for the five sets of oval spiral inductors designed.

Set of Inductors	N, turns	D_o, mm	d_o, mm	w, mm	s, mm	L Formula (12), µH	L Q3D Extractor, µH	Error, %
1st	8	20	10	0.3	0.25	0.839	0.773	8.54
	10	20	10	0.25	0.2	1.229	1.159	6.04
	12	20	10	0.2	0.15	1.969	1.820	8.19
	16	20	10	0.2	0.1	2.545	2.610	2.49
2nd	7	30	15	0.5	0.5	0.895	0.833	7.44
	9	30	15	0.4	0.35	1.516	1.421	6.69
	12	30	15	0.3	0.3	2.282	2.227	2.47
	15	30	15	0.25	0.2	4.021	3.870	3.90
3rd	8	40	20	0.8	0.3	1.609	1.492	7.84
	10	40	20	0.6	0.3	2.402	2.249	6.80
	12	40	20	0.5	0.3	2.954	2.973	0.64
	16	40	20	0.4	0.2	5.089	5.229	2.68

Table 14. *Cont.*

Set of Inductors	N, turns	D_o, mm	d_o, mm	w, mm	s, mm	L Formula (12), μH	L Q3D Extractor, μH	Error, %
4th	7	60	30	1.1	0.8	1.915	1.756	9.05
	9	60	30	0.9	0.6	2.986	2.805	6.45
	12	60	30	0.7	0.4	5.389	5.088	5.92
	15	60	30	0.5	0.4	8.043	7.741	3.90
5th	8	80	40	1.4	0.9	3.038	2.864	6.08
	10	80	40	1.2	0.6	4.804	4.553	5.51
	12	80	40	0.8	0.75	6.550	6.369	2.84
	16	80	40	0.8	0.4	10.180	10.461	2.69

8. Conclusions

Achieving an optimal inductor shape according to the geometry of the device in which it will be used as a component is a complex, specific, particular, difficult, and challenging task. After extensive studies, analytical and numerical analysis, and constructions and experimental measurements, in this article, a new shape of planar spiral inductor is designed. For this new oval shape, the inductance calculation formula used for the classic shapes was adapted. The new inductance formula for the oval planar spiral inductor was validated through both numerical modelling and experimental approaches. The errors between the inductances obtained using the new adapting formula and experimental measurements for the five sets of oval spiral inductors are very small, ranging from 0.57% to 6.25%, with similarly small errors between the analytical and numerical comparisons, ranging from 0.64% to 9.05%. New geometry coefficients based on the current sheet method and experimental tests are developed. These small errors demonstrate the accuracy of the new formula and validate the new geometric coefficients for the oval shape spiral inductors. Moreover, comparative results between the new oval shape and the conventional shapes (square, hexagonal, octagonal, and circular) show a significant increase in inductance, which provides high performance for any device in which it will be used as a component. We are now confident that using the new oval shape results in significantly higher inductance. In accordance with this, the authors aim, in their further research activities, to design a WTP system for pacemakers using these new oval planar spiral inductors, based on the prototype previously constructed with square and circular inductors. The major contributions detailed in this article are a new shape for spiral inductors (the oval shape); a new formula for inductance calculation; and new geometric coefficients required in the inductance formula for the designed and validated shape. The newly designed oval shape offers major advantages compared to conventional shapes, the most important of which is its significant increase in the inductance of the planar spiral inductor. The introduction of the oval-shaped spiral inductors, the newly derived formula for inductance calculation, and the tailored geometric coefficients offer several significant benefits to engineers and researchers. The manuscript outlines several notable benefits for engineers and researchers stemming from the introduction of oval-shaped spiral inductors, the newly developed inductance calculation formula, and the customized geometric coefficients.

Author Contributions: Conceptualization, C.P.; methodology, C.P.; software, C.P., A.G. and C.C.; validation, C.P., V.T., C.M. and A.G.; formal analysis, C.P., A.G., C.C., M.G. and S.A.; investigation, C.P., V.T., C.M., A.G., C.C., M.G. and S.A.; resources, M.G. and S.A.; data curation, C.P., A.G., C.C., V.T., C.M., M.G. and S.A.; writing—original draft preparation, C.P.; writing—review and editing, C.P., A.G. and C.C.; visualization, C.M., C.C., M.G. and S.A.; supervision, V.T.; project administration, A.G.; funding acquisition, A.G. All authors have read and agreed to the published version of the manuscript.

Funding: This research was funded by the Technical University of Cluj-Napoca and by the Academy of Romanian Scientists.

Data Availability Statement: Data are contained within the article.

Acknowledgments: This work was supported with a grant from the Academy of Romanian Scientists, project title: Digitalization of the Evaluation Process of Human Exposure to Electric and Magnetic Fields.

Conflicts of Interest: The authors declare no conflicts of interest.

References

1. Song, Z.C.; Zhou, B. Miniaturized lumped quadrature hybrid using inductance- and integration-enhanced inductors for VHF band applications. *Int. J. RF Microw. Comput.-Aided Eng.* **2022**, *32*, e23431. [CrossRef]
2. Hueil, S.G. RF spiral planar inductor designs—Preliminary results. In Proceedings of the Asia-Pacific Conference on Applied Electromagnetics, 2023, APACE 2003, Shah Alam, Malayasia,, 12–14 August; 2003.
3. Niknejad, A.M.; Meyer, R.G. Analysis, design and optimization of spiral inductors and transformers for Si RFIC's. *IEEE J. Solid State Circuits* **1998**, *33*, 1470–1481. [CrossRef]
4. Constantinescu, C.; Andreica, S.; Laszlo, R.; Giurgiuman, A.; Gliga, M.; Munteanu, C.; Pacurar, C. Numerical Modeling, Analysis, and Optimization of RFID Tags Functioning at Low Frequencies. *Appl. Sci.* **2024**, *14*, 9544. [CrossRef]
5. Eroglu, A. Planar Inductor Design for High Power Applications. *Prog. Electromagn. Res. B* **2011**, *35*, 53–67. [CrossRef]
6. Murugesan, K.S.; Chernobryvko, M.; Zinal, S.; Rossi, M.; Ndip, I.; Boettcher, M.; Lang, K.D.; Wieland, M.; Goetze, C.; Halim, S.B.; et al. High Quality Integrated Inductor in Fan-out Wafer-Level Packaging Technology for mm-Wave Applications. In Proceedings of the 50th European Microwave Conference (EuMC), Utrecht, The Netherlands, 12–14 January 2021; pp. 89–92.
7. Hitzemann, M.; Lippmann, M.; Trachte, J.; Nitschke, A.; Burckhardt, O.; Zimmermann, S. Wireless Low-Power Transfer for Galvanically Isolated High-Voltage Applications. *Electronics* **2022**, *11*, 923. [CrossRef]
8. Chen, X.; Zhang, G.X. Middle range wireless power transfer systems with multiple resonators. *J. Cent. South Univ.* **2015**, *22*, 2127–2136. [CrossRef]
9. Pacurar, C.; Topa, V.; Giurgiuman, A.; Munteanu, C.; Constantinescu, C.; Gliga, M.; Andreica, S. The Construction of a Wireless Power Supply System using Planar Spiral. In Proceedings of the 8th International Conference on Modern Power Systems (MPS), Cluj Napoca, Romania, 21–23 May 2019.
10. Hui SY, R.; Yang, Y.; Zhang, C. Wireless power transfer: A paradigm shift for the next generation. *IEEE J. Emerg. Sel. Top. Power Electron.* **2023**, *11*, 2412–2427. [CrossRef]
11. Wang, K.; Zeng, J.; Yang, Y.; Hui, S.Y.R. A general maximum energy efficiency tracking scheme for domino wireless power transfer systems with quasi-load independent outputs. *IEEE Trans. Power Electron.* **2024**, *39*, 1840–1852. [CrossRef]
12. Shang, S.; Yang, J.; Ji, T.; Fan, M.; Wang, K.; Wang, H. Investigations of A Simplified PCB-Based Wireless Power Resonator Operating at 13.56MHz. In Proceedings of the 2024 10th International Conference on Power Electronics Systems and Applications (PESA), Hong Kong, China, 5–7 June 2024; pp. 1–6.
13. Zhang, C.; Guo, L.; Wang, L.-F.; Huang, J.-Q.; Huang, Q.-A. Passive wireless integrated humidity sensor based on dual-layer spiral inductors. *Electron. Lett.* **2014**, *50*, 1287–1289. [CrossRef]
14. Nieuwoudt, A.; Massoud, Y. Optimizing the Design of Tunable Spiral Inductors for On-Chip Wireless Applications. In Proceedings of the IEEE Annual Wireless and Microwave Technology Conference, Clearwater Beach, FL, USA, 4–5 December 2006; pp. 1–5.
15. Kanaan, A.I.; Sabaawi, A.M.A. *Implantable Wireless Systems: A Review of Potentials and Challenges, Antenna Systems*; IntechOpen: London, UK, 2022.
16. Farooq, M.; Amin, B.; Elahi, A.; Wijns, W.; Shahzad, A. Planar Elliptical Inductor Design for Wireless Implantable Medical Devices. *Bioengineering* **2023**, *10*, 151. [CrossRef] [PubMed]
17. Erokhin, V.V.; Zavyalov, S.A. Optimization of Integrated Inductor Coil Topologies for the Synthesis of Microwave LC Filters in Si/SiGe/GaAs Systems on a Chip. *Vestn. SibSUTI* **2023**, *17*, 87–105.
18. Sheng-Fan, Y.; Tzuen-Hsi, H. Design of Single-Turn Spiral Inductors with Embedding a Strong-Coupling LC Resonator for Interference Suppression. *IEEE Trans. Electromagn. Compat.* **2017**, *59*, 919–926.
19. Pieters, P.; Vaesen, K.; Brebels, S.; Mahmoud, S.F.; De Raedt, W.; Beyne, E.; Mertens, R.P. Accurate modeling of high-Q spiral inductors in thin-film multilayer technology for wireless telecommunication applications. *IEEE Trans. Microw. Theory Tech.* **2001**, *49*, 589–599. [CrossRef]
20. Saberhosseini, S.S.; Ganji, B.A.; Razeghi, A.; Mahmoudi, Z. Modeling & simulation of MEMS spiral inductor. In Proceedings of the 24th Iranian Conference on Electrical Engineering (ICEE), Shiraz, Iran, 10–12 May 2016; pp. 507–510.
21. Raghunadh, M.V.; Abhay Narasimha, K.S. Geometry Optimization of Planar Spiral Inductors operating at 5G mid-band frequencies. In Proceedings of the IEEE International Conference for Innovation in Technology (INOCON), Bangluru, India, 6–8 November 2020; pp. 1–8.

22. Pacurar, C.; Topa, V.; Munteanu, C.; Racasan, A.; Hebedean, C. Studies of Inductance Variation for Square Spiral Inductors using CIBSOC Software. *Environ. Eng. Manag. J.* **2013**, *12*, 1161–1169. [CrossRef]
23. Pacurar, C.; Topa, V.; Giurgiuman, A.; Munteanu, C.; Constantinescu, C.; Gliga, M.; Andreica, S. High Frequency Analysis and Optimization of Planar Spiral Inductors Used in Microelectronic Circuits. *Electronics* **2021**, *10*, 2897. [CrossRef]
24. Grover, F.W. *Inductance Calculations: Working Formulas and Tables*; Van Nostrand: New York, NY, USA, 1946.
25. Mohan, S.S.; Hershenson, M.D.; Boyd, S.P.; Lee, T.H. Simple accurate expressions for planar spiral inductances. *IEEE J. Solid-State Circuits* **1999**, *34*, 1419–1424. [CrossRef]
26. Ammouri, A.; Belloumi, H.; Salah, T.B.; Kourda, F. Experimental analysis of planar spiral inductors. In Proceedings of the 2014 International Conference on Electrical Sciences and Technologies in Maghreb (CISTEM), Tunis, Tunisia, 3–6 November 2014; pp. 1–5.
27. Hussain, I.; Woo, D.-K. Self-Inductance Calculation of the Archimedean Spiral Coil. *Energies* **2022**, *15*, 253. [CrossRef]
28. Greenhouse, H. Design of Planar Rectangular Microelectronic Inductors. *IEEE Trans. Parts, Hybrids, Packag.* **1974**, *10*, 101–109. [CrossRef]
29. Wheeler, H. Simple Inductance Formulas for Radio Coils. *Proc. IRE* **1928**, *16*, 1398–1400. [CrossRef]
30. Faria, A.; Marques, L.; Gaspar, J.; Alves, F. High precision, geometry independent analytical method for self-inductance calculation in planar coils. In Proceedings of the IEEE International Conference on Industrial Technology, Valencia, Spain, 10–12 March 2021; pp. 1234–1239.
31. Beryl, R.; Vaithianathan, V.; Kirubaveni, S. Comparative analysis of various on-chip spiral inductors. In Proceedings of the International Conference on Communication and Signal Processing, Melmaruvathur, India, 3–5 April 2013; pp. 437–441.
32. Gliga, M.; Racasan, A.; Munteanu, C.; Andreica, S.; Pacurar, C.; Topa, V.; Constantinescu, C. The Influence of Ferrite on the Spiral Inductors Inductance used for the Design of Wireless Power Systems. In Proceedings of the International Conference on Modern Power Systems (MPS), Cluj-Napoca, Romania, 6–9 June 2017.
33. Faria, A.; Marques, L.; Ferreira, C.; Alves, F.; Cabral, J. A Fast and Precise Tool for Multi-Layer Planar Coil Self-Inductance Calculation. *Sensors* **2021**, *21*, 4864. [CrossRef] [PubMed]
34. Menicanin, A.; Lukovic, M.; Blaz, N.; Movrin, D.; Zivanov, L. Design and Fabrication of Ferrite Inductor Using 3D Printed Spiral Coil and Ferrite Disc. In Proceedings of the IEEE EUROCON 2019—18th International Conference on Smart Technologies, Novi Sad, Serbia, 1–4 July 2019; pp. 1–4.

Disclaimer/Publisher's Note: The statements, opinions and data contained in all publications are solely those of the individual author(s) and contributor(s) and not of MDPI and/or the editor(s). MDPI and/or the editor(s) disclaim responsibility for any injury to people or property resulting from any ideas, methods, instructions or products referred to in the content.